Electronic Supplementary Material (ESI) for RSC Advances.

DFT Study of Ethanol Dehydration Catalysed by Hematite

Juliana F. Lopes[a], Juliana C. M. Silva[b], Maurício T.M. Cruz[c], José Walkimar de M. Carneiro[d], Wagner B. De Almeida[d,*]

[a] Laboratório de Química Computacional (LaQC), Instituto de Física e Química,Universidade Federal de Itajubá (UNIFEI), Av. BPS, 1303 Pinheirinho, Itajubá, MG, 37500-903, Brazil.

[b] Departamento de Química, ICEx, Universidade Federal de Minas Gerais (UFMG), Campus Pampulha, Belo Horizonte, MG, 31270-901, Brazil.

[c] Instituto de Química, Universidade do Estado do Rio de Janeiro (UERJ), Rua São Francisco Xavier, 524, Pavilhão Haroldo Lisboa da Cunha, Maracanã, Rio de Janeiro, RJ, 20550-900, Brazil.

[d] Laboratório de Química Computacional (LQC), Departamento de Química Inorgânica, Instituto de Química, Universidade Federal Fluminense (UFF), Campus do Valonguinho, Centro, Niterói, RJ, CEP: 24020-141, Brazil

SUPPLEMENTARY MATERIAL

Table S1. MP2/6-31G(d,p) geometrical parameters[a] for the molecular species present in the gas-phase ethanol dehydration process, according to Scheme 1 (See Figure 5b for atom numbering).

Bond/Angle	Ethanol	Transition State	Product
C1-C2 (Å)	1.52 (1.53) [a]	1.42 (1.42) [a]	1.34 (1.33) [a]
C1-O7 (Å)	1.43 (1.43) [a]	1.82 (1.86) [a]	3.44 (3.44) [a]
C2-H9 (Å)	1.09 (1.09) [a]	1.46 (1.44) [a]	2.51 (2.51) [a]
H9-C2-C1 (°)	110.1 (110.4) [a]	72.6 (73.8) [a]	74.6 (74.6) [a]
H3-C2-H6 (°)	107.9 (107.6) [a]	116.0 (115.5) [a]	117.0 (116.7) [a]
C2-C1-O7 (°)	112.4 (112.7) [a]	95.0 (94.0) [a]	78.7 (78.8) [a]
C2-C1-O7-H8 (°)	62.8 (62.5) [a]	103.8 (105.6) [a]	94.5 (94.6) [a]

[a] The B3LYP/6-31G(d,p) values a given in parenthesis.

Table S2. *Ab initio* gas-phase relative energies and thermodynamic properties (p = 1 atm; T = 298 K) for molecular species present in the ethanol dehydration process (Scheme 1). All values in kcal mol^{-1}.

Gas Phase	**Ethanol**	**TS structure**			**Ethylene + Water**		
		$\Delta E^{\ddagger}$	$\Delta H^{\ddagger}$	$\Delta G^{\ddagger}$	ΔE	ΔH	ΔG
B3LYP/6-31G(d,p)	0.0	69.6	64.5	69.7	18.2	16.4	10.6
B3LYP/6-31++G(d,p)//B3LYP/6-31G(d,p)	0.0	67.7	62.6	67.8	13.3	11.5	5.7
B3LYP/6-311++G(2d,2p)//B3LYP/6-31G(d,p)	**0.0**	**67.6**	**62.5**	**67.7**	**10.7**	**8.9**	**3.1**
B3LYP/6-311++G(3df,3pd)//B3LYP/6-31G(d,p)	0.0	67.5	62.4	67.6	10.8	9.0	3.2
B3LYP/aug-cc-pVTZ//B3LYP/6-31G(d,p)	0.0	67.3	62.2	67.4	10.7	8.9	3.1
PBE1PBE/6-31G(d,p)//B3LYP/6-31G(d,p)	0.0	70.9	-	-	21.9	-	-
PBE1PBE/6-31++G(d,p)//B3LYP/6-31G(d,p)	0.0	69.2	-	-	17.6	-	-
PBE1PBE/6-311++G(2d,2p)//B3LYP/6-31G(d,p)	0.0	69.1	-	-	15.5	-	-
CAM-B3LYP/6-31G(d,p)//B3LYP/6-31G(d,p)	0.0	72.6			21.2		
CAM-B3LYP/6-31++G(d,p)//B3LYP/6-31G(d,p)	0.0	70.8			16.1		
CAM-B3LYP/6-311++G(2d,2p)//B3LYP/6-31G(d,p)	0.0	70.6			13.5		
M062x/6-31G(d,p)//B3LYP/6-31G(d,p)	0.0	73.7	-	-	20.4	-	-
M062x/6-31++G(d,p)//B3LYP/6-31G(d,p)	0.0	72.0	-	-	16.5	-	-
M062x/6-311++G(2d,2p)//B3LYP/6-31G(d,p)	0.0	71.9	-	-	14.2	-	-
MP2/6-31G(d,p)	0.0	74.8 (75.0)[a]	69.5 (69.8)[a]	64.7 (75.0)[a]	17.2 (17.2)[a]	14.9 (15.3)[a]	9.2 (9.6)[a]
MP2/6-31++G(d,p)//MP2/6-31G(d,p)	0.0	71.8	66.5	61.7	13.0	10.7	5.0
MP2/6-311++G(2d,2p)//MP2/6-31G(d,p)	0.0	70.1	64.8	60.0	11.0	8.7	3.0
MP4(SDTQ)/6-31G(d,p)//MP2/6-31G(d,p)	0.0	85.8	80.5	75.7	16.42	14.1	8.4
MP4(SDTQ)/6-31++G(d,p)//MP2/6-31G(d,p)	0.0	72.3	67.0	62.2	12.7	10.4	4.7
MP4(SDTQ)/6-311++G(2d,2p)//MP2/6-31G(d,p)	0.0	70.3	65.0	60.2	10.7	8.4	2.7
CCSD(T)/6-31G(d,p)//MP2/6-31G(d,p)	0.0	75.9	70.6	65.8	15.4	13.1	7.4
CCSD(T)/6-31++G(d,p)//MP2/6-31G(d,p)	0.0	73.3	68.0	66.8	11.8	9.8	4.1
CCSD(T)/6-311++G(2d2,p)//MP2/6-31G(d,p)	**0.0**	**71.8**	**66.5**	**61.7**	**10.2**	**7.9**	**2.2**

[a] MP2/6-31G(d,p)//B3LYP/6-31G(d,p) value.

Table S3. MP2/6-311++G(2d,2p)//B3LYP/6-31G(d,p) thermodynamic properties as function of temperature for the gas-phase ethanol dehydration process according to Scheme 1.

Temperature (K)	$\Delta G°$ (kcal mol^{-1})	$\Delta H°$ (kcal mol^{-1})	$T\Delta S$ (kcal mol^{-1})	$\Delta G^{‡}$ (kcal mol^{-1})	$\Delta H^{‡}$ (kcal mol^{-1})	$T\Delta S^{‡}$ (kcal mol^{-1})	k (s^{-1})
300	3.3	9.1	5.8	65.1	64.9	-0.17	2.3×10^{-35}
350	2.3	9.4	7.1	65.1	65.0	-0.16	1.6×10^{-28}
400	1.3	9.6	8.4	65.2	65.0	-0.12	2.1×10^{-23}
450	0.2	9.8	9.6	65.2	65.1	-0.08	2.1×10^{-19}
500	-0.9	10.1	10.9	65.2	65.1	-0.03	3.4×10^{-16}
550	-2.0	10.3	12.2	65.2	65.2	0.03	1.5×10^{-13}
600	-3.1	10.4	13.5	65.2	65.2	0.08	2.3×10^{-11}
650	-4.2	10.6	14.8	65.2	65.3	0.13	1.7×10^{-9}
700	-5.4	10.7	16.0	65.1	65.3	0.18	6.7×10^{-8}
750	-6.5	10.8	17.3	65.1	65.4	0.23	1.6×10^{-6}
800	-7.7	10.9	18.6	65.1	65.4	0.27	2.7×10^{-5}
850	-8.8	11.0	19.8	65.1	65.4	0.30	3.2×10^{-4}
900	-10.0	11.0	21.0	65.1	65.4	0.33	2.9×10^{-3}
950	-11.2	11.1	22.3	65.1	65.4	0.35	2.1×10^{-2}
1000	-12.3	11.2	23.5	65.0	65.4	0.37	1.3×10^{-1}
1050	-13.5	11.2	24.7	65.0	65.4	0.38	0.64
1100	-14.7	11.2	25.9	65.0	65.4	0.39	2.8
1150	-15.9	11.3	27.1	65.0	65.4	0.39	10.7
1200	-17.0	11.3	28.3	65.0	65.4	0.38	36.7

Table S4. Relative energies (kcal mol^{-1}) for Fe_2O_3 linear neutral monomer.

Spin Multiplicity (2S+1)	UB3LYP/ 6-31(d,p)	UB3LYP/ 6-311++G(d,p)// UB3LYP/ 6-31(d,p)	UMP2/ 6-31G(d,p)	UMP2/ 6-311++G(2d,2p)// UMP2/ 6-31G(d,p)	UMP4(SDTQ)/ 6-311++G(2d,2p)// U MP2/ 6-31G(d,p)	UCCSD(T)/ 6-311++G(2d,2p)// U MP2/ 6-31G(d,p)
1	91.1	91.9	-	-	-	-
3	66.2	87.5	-	-	-	-
5	24.4	22.2	88.8	113.4	113.9	-
7	**0**	47.6	17.9	22.1	29.4	19.3
9	38.3	88.4	23.7	31.0	31.0	22.4
11	**5.2**	**0**	**0**	**0**	**0**	**0**
13	54.3	48.9	140.9	147.9	-	-
15	167.2	162.2	157.4	171.3	-	-
17	308.6	306.6	302.5	332.3	-	-

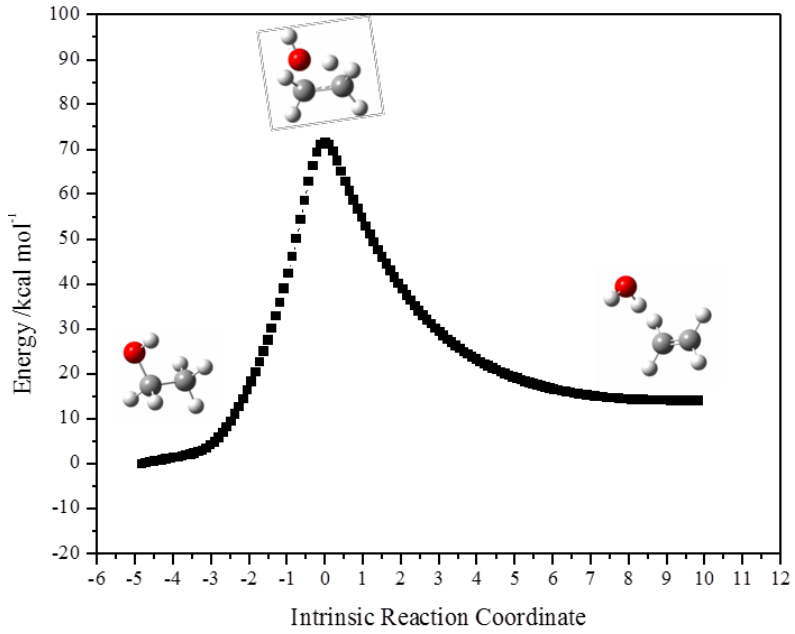

(a) MP2/6-31G(d,p) IRC curve.

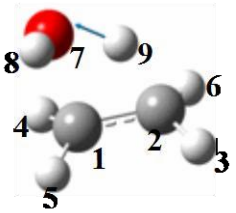

(b) Displacement vectors of the MP2/6-31G(d,p) imaginary frequency mode of the TS structure

Figure S1. MP2/6-31G(d,p) IRC for the gas-phase ethanol dehydration process according to Scheme 1 (a) and displacement vectors of the transition state imaginary frequency mode (2080i cm^{-1}; MP2/6-31G(d,p) value) (b).

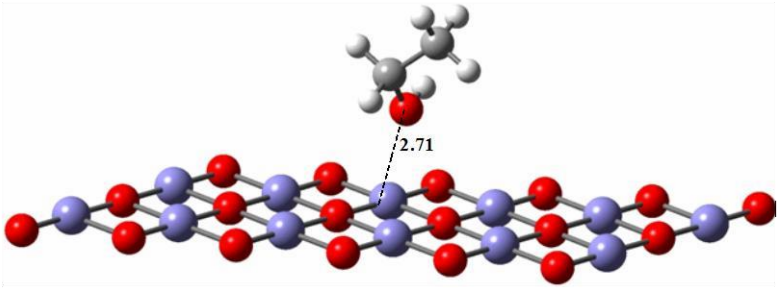

(a)

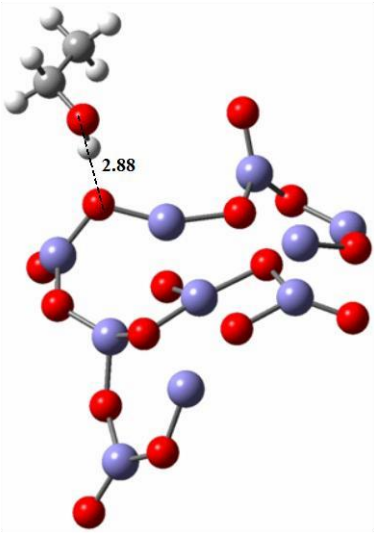

(b)

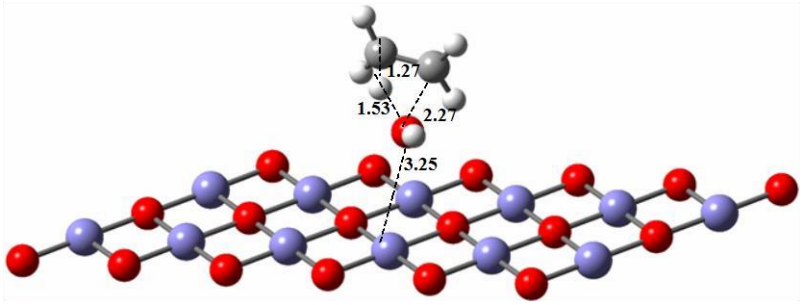

(c)

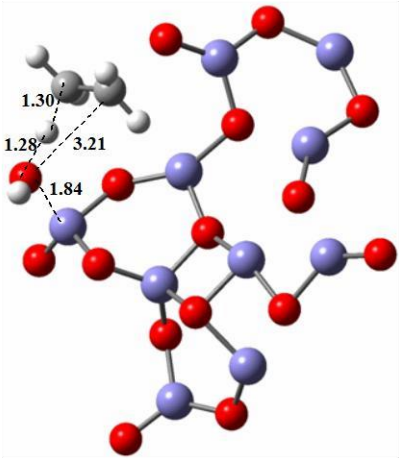

(d)

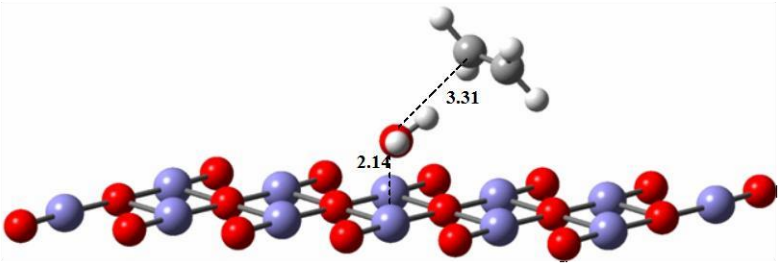

(e)

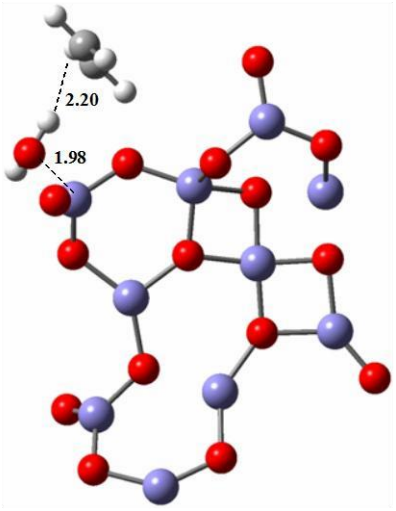

(f)

Figure S2. UB3LYP/6-31G(d,p) optimized undecet spin state catalyst structures.
(a) $Fe_{12}O_{18}$ planar (Reactant) (b) $Fe_{10}O_{15}$ non-planar (Reactant)
(c) $Fe_{12}O_{18}$ planar (TS) (d) $Fe_{10}O_{15}$ non-planar (TS)
(a) $Fe_{12}O_{18}$ planar (Product) (b) $Fe_{10}O_{15}$ non-planar (Product)

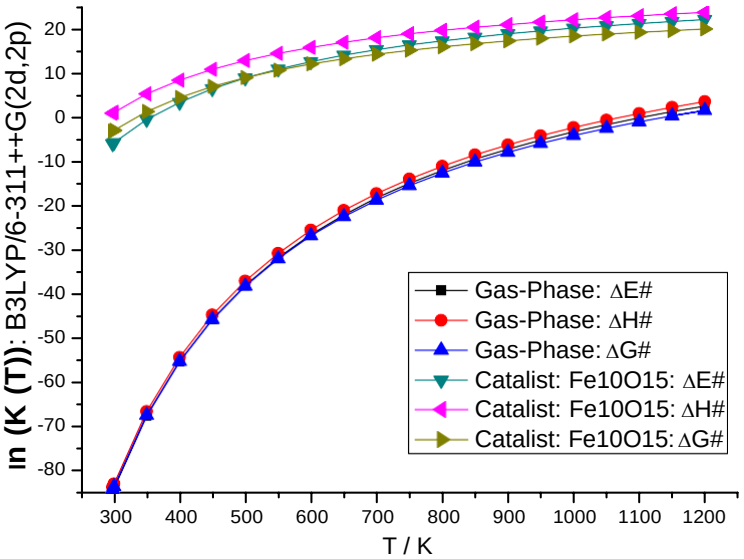

Figure S3. A comparison between B3LYP/6-311++G(2d,2p)//B3LYP/6-31G(d,p) rate constant (lnk(T)) profiles for the ethanol dehydration gas phase and catalytic ($Fe_{10}O_{15}$ singlet state) process, using $\Delta E^{\#}$, $\Delta H^{\#}$ and $\Delta G^{\#}$ values in equation (2) for the evaluation of k(T).